JCTC Journal of Chemical Theory and Computation

Article

pubs.acs.org/JCTC

Applications of Polarizable Continuum Models To Determine Accurate Solution-Phase Thermochemical Values Across a Broad Range of Cation Charge – The Case of U(III–VI)

Payal Parmar,* Alex Samuels, and Aurora E. Clark*

Department of Chemistry and the Materials Science and Engineering Program, Washington State University, Pullman, Washington 99164, United States

Supporting Information

ABSTRACT: Contributing factors to the solution-phase correction to the free energy of the molecular clusters $U(H_2O)_n^{3+/4+}$ and $UO_2(H_2O)_m^{1+/2+}$ (n = 8, 9, 30, 41, 77; m = 4, 5, 30, 41, 77) have been examined as a function of cavity type in the integrated-equation-formalism-protocol (IEF) and SMD polarizable continuum models (PCMs). It is observed that the free energy correction, G_{corr}, does not smoothly converge to zero as the number of explicitly solvating water molecules approaches the bulk limit, and the convergence behavior varies significantly with cavity and model. The rates of convergence of the gas-phase hydration energy, ΔG_{hyd}, wherein the bare metal ion is inserted into a molecular water cluster and ΔG_{corr} for the reaction exhibit wide variations as a function of ion charge, cavity, and model. This is the likely source of previously reported discrepancies in predicted free energies of solvation for metal ions when using different PCM cavities and/or models. The cancellation of errors in ΔG_{hyd} and ΔG_{corr} is optimal for clusters consisting of only a second solvation shell of explicit water molecules (n = m = 30). The UFF cavity within IEF, in particular, exhibits the most consistent cancellation of errors when using a molecular cluster consisting of a second shell of solvating water for all oxidation states of uranium, leading to accurate free energies of solvation ΔG_{solv} for these species.

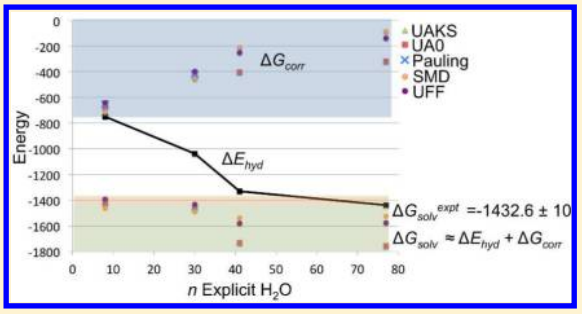

INTRODUCTION

Polarizable continuum models (PCMs) have become an increasingly useful tool for predicting the electronic structures of ground and excited states as well as the geometries of molecules in solution.[1−4] Their application for predicting accurate solution-phase thermochemical values has been thoroughly examined for organic and small molecules, wherein a general utility has been demonstrated.[5] Several studies have utilized PCMs to closely reproduce the experimental solvation free energies of neutral and ionic organic species.[6−10] In the case of cations and polar media, the comparably stronger solute−solvent interactions often leads to use of a molecular cluster model wherein explicit solvent molecules are added to mimic the ion's immediate solvation environment. The aqueous chemistry of cations is emphasized in the literature as it is relevant to many disciplines that span the biological and technological sectors. In this case, a hydrated cluster is then embedded within the continuous dielectric. This approach represents the intersection of the continuum approach and discrete solvation models, yet it is bolstered by the general acceptance[11] that such hydrated cations exist in solution as metastable and dynamically evolving species (meaning that a specific solvation configuration has a measurable lifetime in solution and can be considered a distinct molecular species). Within embedded molecular cluster models, gas-phase optimizations are often performed, followed by further refinement of the geometry of the molecular cluster using the PCM.[12,13] It has been observed that the PCM optimized geometries are quite sensitive to the continuum solvation model. Further the solvation contribution to the free energies of many metal cations has been demonstrated to be highly sensitive to the size of the molecular cluster and the continuum model and or cavity.[14,15]

For many ions the aqueous thermochemistry is particularly important, as they may exhibit complex speciation that in turn influences reactivity. Nowhere is this more evident than in the actinide (An) cations, which not only exhibit solvation coordination environments that are highly sensitive to aqueous conditions but also complex equilibria between oxidation states, with the possibility that several oxidation states coexist in solution. In this scenario, large changes in the electrostatic interaction between the ion and water necessitate a molecular cluster model with an appropriate number of explicit waters to be paired with a PCM that can adequately describe multiple oxidation states. While prior work has demonstrated that solution-phase cation thermochemistry can depend upon the number of explicit water molecules and the continuum model,[15,16] no systematic investigation has examined the physical premise of this behavior or its sensitivity to ion

Received: June 19, 2014
Published: December 8, 2014

   dx.doi.org/10.1021/ct500530q | J. Chem. Theory Comput. 2015, 11, 55−63

charge. This is particularly relevant as most PCM's have been parametrized in the absence of explicit solvent molecules and using ions of low charge.[1,17−26]

Toward this end a series of hydrated uranium ion clusters has been examined, where the metal oxidation state is varied from III to VI, leading to molecular cluster charges that span +4 to +1. A computational approach has been used that encompasses the reactions

$$U^{3+/4+} + (H_2O)_n \rightarrow U(H_2O)_n^{3+/4+}$$

$$UO_2^{1+/2+} + (H_2O)_n \rightarrow UO_2(H_2O)_n^{+/2+}$$

that represent the hydration reactions of the bare ions (note that U^{5+} and U^{6+} rapidly react with O_2 or H_2O to form the linear diyl cations, which are the predominant chemical species). Gas-phase calculations determine the free energy for this process, ΔG_{hyd}, followed by single point PCM calculations that determine the solvation correction (G_{corr}) to the $(H_2O)_n$ and hydrated metal cluster so as to determine the solution-phase free energy for the reaction, which is called the free energy of solvation, ΔG_{solv}, for ion. Note that the bare ion is left in the gas-phase as this is consistent with the experimental calorimetry approximations associated with the heat released from dissolving the ion containing salt.[27] Further, a cluster of hydrogen bonded water should be employed so as to avoid imbalances in the hydrogen bond network of the reactants and products.[15,28] A "standard state" correction, SS_{corr}, may also be applied; however, it is quite small relative to the other two terms if a hydrogen bonded cluster is employed.[29] The SS_{corr} is generally based upon the quasi-chemical method and is a measure of the reversible work of coupling the solute with the solvent (also referred to as the Ben-Naim definition), which amounts −4.3/n kcal/mol for each $(H_2O)_n$ water cluster).[30,31] The total solution-phase free energy of solvation is then

$$\Delta G_{solv} = \Delta G_{hyd} + \Delta G_{corr} + SS_{corr} \quad (1)$$

The implementation of the calculation of ΔG_{solv} in a thermochemical cycle is presented in Figure S1 in the Supporting Information. The errors associated with this approach are a composite deriving from ΔG_{hyd} as well as ΔG_{corr}. Errors in the gas-phase energetics may derive from either the method or the basis set or other approximations including those associated with relativistic effects. The cluster model employed to define the explicit solvation environment about the ion also influences both the gas- and solution-phase calculations. A variational approach for determining the optimal cluster size has been previously developed.[32] Yet, for clusters of infinite size (the bulk limit) ΔG_{hyd} is equivalent to ΔG_{solv}, and the solvation correction ΔG_{corr} for the reaction should go to zero. Unfortunately, different convergence properties may be observed for the gas-phase energetics and solvation corrections which may contribute to the aforementioned deviations in ΔG_{solv} as a function of system size and continuum model.

The underlying premise of the current work is to first establish that the typical gas-phase computational protocols for determining thermochemistry of An ions represents a sound basis for subsequent solution-phase corrections determined by the PCM approach and then to investigate the performance of different models and cavities as a function of cation charge and the number of explicit water molecules utilized in the molecular cluster. This is of paramount importance because the solvation correction can be nearly 50% of the total free energy of solvation (vide infra). The current work enables a better understanding of the contributing factors to the solvation correction which bears on the performance of previously reported variational approaches for determining optimal cluster size.[32] Very different convergence properties are observed for the gas-phase hydration energies and the solvation corrections, often leading to an imbalance in cancellation that leads to large errors in the resulting free energies of solvation. This indicates that there may be instances when the cluster-continuum scheme does not obey the variational principle. Within the systems studied here, favorable cancellation of errors is consistently observed across all systems when using the UFF cavity within the IEF model for chemical reactions wherein the chemical model consists of a molecular cluster with two explicit solvation shells.

COMPUTATIONAL METHODOLOGY

Significant prior work[15,16,33−37] has established that ΔG_{hyd} of f-element ions is relatively insensitive to the density functionals within those that form the so-called rungs on the Jacob's ladder[38,39] of density functionals. The range of ΔG_{hyd} for Ln(III) with varying density functional is generally ∼5 kcal/mol using a double-ζ basis set on H_2O and a small-core relativistically corrected effective core potential (SC-RECP) on the metal. However, ΔG_{hyd} can be quite sensitive to the basis set, particularly that of the metal, with large variations observed depending on whether a small- or large-core RECP is used, the latter resulting in significant underestimations of the reaction energy.[15] A double-ζ quality basis set for the O- and H atoms of water has been observed to result in consistent quality ΔG_{hyd} for actinide and lanthanide (Ln) ions.[15,40] While SC-RECPs are generally considered to be of sufficient quality for determining ΔG_{hyd}, recent developments in the valence basis sets for uranium contain *g*-functions, which play important role in the correlation of 5*f*-electrons. It is unclear what practical impact this may have upon gas- or solution-phase thermochemistry. Explicit consideration of relativistic affects is generally not needed for most computational applications involving local minima on the potential energy surface of An bearing species;[34,35,37,41] however, the role of spin−orbit coupling upon the energetics of hydrated species may gain importance because explicitly solvating water molecules donate their electron density to the ion center, potentially increasing the *f*-orbital occupation. Taking these issues into account, the gas-phase free energies of hydration (ΔG_{hyd}) were first calculated for the reactions

$$U^{3+/4+} + (H_2O)_{8,9} \rightarrow U(H_2O)_{8,9}^{3+/4+} \quad (r1)$$

$$U^{3+/4+} + (H_2O)_{30} \rightarrow U(H_2O)_{8,9}(H_2O)_{22,21}^{3+/4+} \quad (r2)$$

$$UO_2^{1+/2+}(H_2O)_{4,5} \rightarrow UO_2(H_2O)_{4,5}^{+/2+} \quad (r3)$$

$$UO_2^{1+/2+} + (H_2O)_{30} \rightarrow UO_2(H_2O)_{4,5}(H_2O)_{26,25}^{1+/2+} \quad (r4)$$

The geometry of each molecular species was optimized using the unrestricted form of the B3LYP[42,43] functional (UB3LYP) using the NWChem[44] software program. Two sets of SC-RECPs[45,46] were employed along with their associated basis sets for valence electrons (*vide infra*). The aug-cc-pVDZ basis set was employed for the H- and O atoms of clusters that contained a single solvation shell (4−9 H_2O), while for those

dx.doi.org/10.1021/ct500530q | J. Chem. Theory Comput. 2015, 11, 55−63

clusters containing 30 H_2O, the 6-311G** basis[47] was used. Geometries of the first solvation shell clusters (in r1 and r3) were optimized employing the contracted as well as uncontracted versions of both basis sets, while the second solvation shell clusters (in r2 and r4) were optimized using the contracted basis with subsequent single point calculations being performed using the uncontracted basis to save computational time. Thermodynamic corrections were obtained from normal-mode analysis, which in addition verified all structures to be actual minima with real frequencies. The contributions of spin−orbit coupling to the reaction energetics were determined from single point spin−orbit DFT (SO−DFT) calculations using the small core RECP[46] of Dolg, which includes the spin−orbit potential functions (SO-ECP). Counter-poise corrections were not included to correct for basis set superposition error, as prior studies have shown that the magnitude of the correction is minimal compared to water binding energies to Ln(III).[48] The thermodynamics of the water addition reactions (ΔG_{add}) to the first solvation shell were then explored using the same methods and basis sets.

$$U(H_2O)_8^{3+/4+} + H_2O \rightarrow U(H_2O)_9^{3+/4+} \quad \text{(r5)}$$

$$U(H_2O)_8(H_2O)_{22}^{3+/4+} \rightarrow U(H_2O)_9(H_2O)_{21}^{3+/4+} \quad \text{(r6)}$$

$$UO_2(H_2O)_4^{1+/2+} + H_2O \rightarrow UO_2(H_2O)_5^{1+/2+} \quad \text{(r7)}$$

$$UO_2(H_2O)_4(H_2O)_{26}^{1+/2+} \rightarrow UO_2(H_2O)_5(H_2O)_{25}^{1+/2+} \quad \text{(r8)}$$

Single point polarizable continuum model (PCM) calculations were performed on all species except the bare ions within reactions r1−r8. The UFF, UA0, UAKS, and Pauling cavities were studied using the integral-equation-formalism-protocol (IEF) implemented in Gaussian03,[49] wherein the cavity is created using a series of overlapping spheres, initially devised by Tomasi and co-workers and Pascual-Ahuir and co-workers.[5,50,51] For the solvent of water, the default settings in Gaussian03 scale the atomic radii in UAKS by $\alpha = 1.2$, with the radii for other cavities unscaled ($\alpha = 1.0$). The IEF model using the radii and nonelectrostatic terms of Truhlar and co-worker's SMD solvation model in Gaussian09 (denoted as SMD) was also examined wherein $\alpha = 1.1$ by default.[52,53] There are two primary differences between the Gaussian03 and Gaussian09 cavities: 1) the former uses point charges, while the latter uses Gaussian charges so that discontinuities in the cavity are avoided (when two point charges on different spheres get to close to each other), and 2) Gaussian03 uses added spheres to fill regions of space that are not accessible to the solvent (for instance, when two spheres on different centers may get close to each other without yet touching), while in Gaussian09 these added spheres are not used because they complicate the equations with the Gaussian charges. For the sake of brevity, the different cavities within IEF will simply be denoted as UFF, UA0, UAKS, and Pauling.

The convergence of the hydration energetics in the gas-phase and in solution was examined via single point calculations for the reactions

$$U^{3+/4+} + (H_2O)_n \rightarrow U(H_2O)_8(H_2O)_{n-8}^{3+/4+} \quad \text{(r9)}$$

$$UO_2^{1+/2+} + (H_2O)_n \rightarrow UO_2(H_2O)_5(H_2O)_{n-5}^{1+/2+} \quad \text{(r10)}$$

where $n = 41$ and 77. The configurations for these very large clusters were obtained using an approach similar to Yang and Bursten,[54] wherein a rigid $U(H_2O)_8^{3+/4+}$ and $UO_2(H_2O)_5^{+/2+}$ molecular species was immersed inside a box of 2039 classical TIP3P[55] water molecules. Atomic charges for the rigid hydrated first solvation shell clusters were obtained using the Mulliken charges obtained by the gas-phase optimization of the second solvation shell species $U(H_2O)_8(H_2O)_{22}^{3+/4+}$ and $UO_2(H_2O)_5(H_2O)_{25}^{+/2+}$. A Lennard-Jones + coulomb potential was used to describe the interaction of the rigid cluster with the bulk TIP3P water. The LJ potential for the interaction of the TIP3P water with the central ion of the $U(H_2O)_8^{3+/4+}$ and $UO_2(H_2O)_5^{+/2+}$ was developed from the two-body dissociative potential energy surface obtained using the program ForceFit,[56] by sequentially lengthening the distance of an arbitrarily chosen second solvation shell cluster in the $U(H_2O)_8(H_2O)_{22}^{3+/4+}$ and $UO_2(H_2O)_5(H_2O)_{25}^{+/2+}$ clusters. The LJ potential between TIP3P water and the solvating water in the cluster was taken from the TIP3P model with the charges of the solvating waters adjusted according to the Mulliken charges of the DFT calculations. The atomic charges, σ and ε, are presented in Table S1 in the Supporting Information. One ns of equilibration in NPT and NVT ensembles was pursued, followed by a 1 ns production run in NVE using the DL_POLY4[57−59] software program. The equilibrated density was 0.998 g/cm^3. A 1 fs time step was used with an ewald cutoff of 9 Å and a threshold of 10^{-8}. The larger water clusters were carved out of 5 representative snapshots of the simulation box by removing a sphere of water within 6.5 and 8.0 Å from the $U^{3+/4+}$ metal center and 6.7 and 8.3 Å from the $UO_2^{1+/2+}$ solute. Five spherical $(H_2O)_{41,77}$ clusters were removed from a similarly equilibrated pure TIP3P water simulation. The specific snapshots were chosen based upon the fact that they each contained the same number of hydrogen bonds, as defined by a geometric criterion of $r < 2.5$ Å and ϕ between 145° and 180° (see Figure S2 in the Supporting Information) and identified by the *ChemNetworks* software program.[60] Each cluster was then subjected to a single point calculation in the gas-phase and with each of the aforementioned dielectric continuum models and cavities using UB3LYP/RSC60/6-311G** (average values reported). This protocol enabled a partial accounting of configurational sampling within the clusters, while it ensured that energetic differences manifested within the solvation free energies as a function of system size were due to changes in the performance of the continuum cavity or model, which was the emphasis of this work. The average error associated with the 5 snapshots chosen was ±3 kcal/mol for the solvation free energies presented.

RESULTS AND DISCUSSION

Gas-Phase Energetics: Basis Sets and Relativistic Effects Using UB3LYP. This section focuses upon the gas-phase ΔG_{hyd} of U(III−VI) as a function of computational approach so as to establish the quality of the gas-phase thermochemistry prior to solvation corrections. The sensitivity of thermodynamic values to the Gaussian basis sets and relativistic effective core potentials employed and the importance of spin−orbit effects have been examined. Representative optimized geometries of the first and nominal second solvation shell structures are presented in Figure 1. For the sake of computational expedience the same number of total waters was maintained for all clusters that encompass more

dx.doi.org/10.1021/ct500530q | J. Chem. Theory Comput. 2015, 11, 55−63

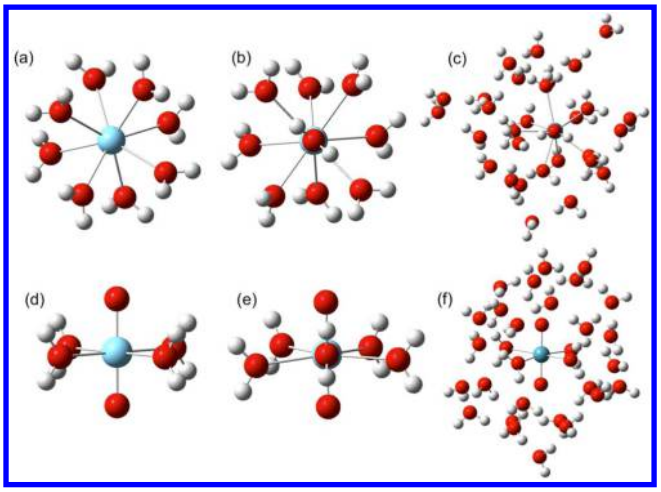

Figure 1. Representative geometries for (a) $U(H_2O)_8^{3+/4+}$, a square antiprism (SAP); (b) $U(H_2O)_9^{3+/4+}$, a tricapped trigonal bipyrimid (TTBP); (c) the solvation shell structure of $U(H_2O)_9(H_2O)_{21}^{3+/4+}$; (d) $UO_2(H_2O)_4^{1+/2+}$; (e) $UO_2(H_2O)_5^{1+/2+}$; (f) the 1st and 2nd solvation shell structure $UO_2(H_2O)_4(H_2O)_{26}^{1+/2+}$.

than the first solvation shell. The ΔG_{hyd} and ΔG_{add} reactions r1 − r8 were first considered.

The small-core, energy-optimized RECP for uranium published in 1994 by the Stuttgart group[45] considers the core to be comprised of 60 electrons (i.e., the 1*s*-4*s*, 2*p*-4*p*, 3*d*-4*d*, and the 4*f* shells) and has been shown to yield comparatively accurate results for geometries and energies.[36,61−63] In order to better describe the correlation of the valence electrons in uranium, *g*-functions in the basis sets are expected to be important, particularly when the 5*f* orbitals actively participate in bonding. In 2009, Dolg and Cao[46] reported a new SC-RECP that improved upon the original 1994 Stuttgart one[45] for uranium by accounting for relativistic behavior more accurately by constructing it using the (two-component) multiconfigurational Dirac-Hartree−Fock (MCDHF) approach as opposed to the Wood-Boring quasi-relativistic approach in the 1994 Stuttgart RECPs. The associated valence basis functions have additionally two *s*-, two *p*-, and six *g*-functions. Therefore, one is required to use the 2009 RECP along with its segmented basis sets for valence electrons for the calculation of a more accurate description of the properties, like spin−orbit contributions, in the uranium systems. For the sake of clarity, the older Stuttgart SC-RECP basis set is referred to as RSC(1994), while the latter is referred to as RSC(2009). Table 1 compares the ΔG_{hyd} as a function of uranium oxidation state using both the contracted and uncontracted forms of RSC(1994) and RSC(2009).

When using the contracted basis sets the ΔG_{hyd} for reactions r1 and r3 is altered on an average by 2.6 kcal/mol when switching from RSC(1994) to RSC(2009). Addition of *g*-functions typically cause an increase in the hydration energy of the tri- and tetravalent as well as the UO_2^{1+} ions (becoming less negative), while the ΔG_{hyd} of the closed shell UO_2^{2+} ion slightly shifted to the more negative. No trend is observed regarding the impact of the *g*-functions upon ΔG_{hyd} as a function of the *f*-orbital occupation of the ion (Figure S3 is given in the Supporting Information). Uncontracting the RSC(1994) basis set generally increases ΔG_{hyd} by about 1.0 kcal/mol on an average, while uncontracting RSC(2009) alters ΔG_{hyd} by ∼1.1 kcal/mol. This is similar to what was observed in prior study[33] of the hydration reactions of the Ln(III) which indicated that the difference in the total electronic energies with the SCF-optimized DFT for La^{3+} and Lu^{3+} cations with small core contracted and uncontracted basis is significantly small provided that there is no major change in the DFT density while uncontracting the basis. The affect of the additional *g*-functions was also examined for hydration reactions that encompass energies for the second solvation shell, reactions r2 and r4, presented in Table S2 in the Supporting Information; however, the same behavior is observed. Thus, the RSC(2009) RECP and basis does not present a significant improvement to the energetics of these ions relative to the oft-used RSC(1994) basis sets.

The influence of basis set may be more important to ΔG_{add} (reactions r5 and r7) because the magnitude of these energies is much smaller than $\Delta G_{hyd,}$ and subtle effects can have a large impact upon the thermodynamically favored coordination environment. As observed in Table 2 for the first solvation shell clusters, the ΔG_{add} values are within 1.0 kcal/mol of each other using either RSC(1994) or RSC(2009). Uncontraction of either basis set also has negligible impact upon the calculated energetics, and similar behavior is observed for the reactions of the second shell hydrated clusters r6 and r9.

Table 1. Gas-Phase ΔG_{hyd} Values (in kcal/mol) for Actinide Hydration (Reactions r1 and r3), Where RSC(1994)-C and RSC(1994)-U Refer to the Contracted and Uncontracted Forms of the RSC(1994) Basis Set and so Forth

		$U^{3+} + (H_2O)_n \rightarrow U(H_2O)_n^{3+}$		
	RSC(1994)-C	*RSC(1994)-U*	*RSC(2009)-C*	*RSC(2009)-U*
n = 8	−397.3	−396.4	−395.5	−394.8
n = 9	−407.1	−406.0	−405.1	−404.7
		$U^{4+} + (H_2O)_n \rightarrow U(H_2O)_n^{4+}$		
	RSC(1994)-C	*RSC(1994)-U*	*RSC(2009)-C*	*RSC(2009)-U*
n = 8	−737.5	−736.1	−732.1	−730.9
n = 9	−760.1	−758.5	−754.9	−753.7
		$UO_2^{+} + (H_2O)_n \rightarrow UO_2(H_2O)_n^{+}$		
	RSC(1994)-C	*RSC(1994)-U*	*RSC(2009)-C*	*RSC(2009)-U*
n = 4	−80.7	−80.4	−79.5	−76.8
n = 5	−84.4	−84.1	−82.4	−81.8
		$UO_2^{2+} + (H_2O)_n \rightarrow UO_2(H_2O)_n^{2+}$		
	RSC(1994)-C	*RSC(1994)-U*	*RSC(2009)-C*	*RSC(2009)-U*
n = 4	−177.2	−179.0	−178.5	−178.7
n = 5	−192.4	−196.3	−194.1	−193.1

dx.doi.org/10.1021/ct500530q | J. Chem. Theory Comput. 2015, 11, 55−63

Table 2. Gas-Phase ΔG_{add} Values (in kcal/mol) for Reactions r5 and r7, Where RSC(1994)-C and RSC(1994)-U Refer to the Contracted and Uncontracted Forms of the RSC(1994) Basis Set and so Forth

	$U(H_2O)_8^{x+} + H_2O \rightarrow U(H_2O)_9^{x+}$			
	RSC(1994)-C	*RSC(1994)-U*	*RSC(2009)-C*	*RSC(2009)-U*
$x = 4+$	−23.6	−23.5	−23.7	−23.8
$x = 3+$	−10.8	−10.6	−10.6	−10.9
	$UO_2(H_2O)_4^{x+} + H_2O \rightarrow UO_2(H_2O)_5^{x+}$			
	RSC(1994)-C	*RSC(1994)-U*	*RSC(2009)-C*	*RSC(2009)-U*
$x = 2+$	−14.3	−15.6	−14.7	−13.3
$x = 1+$	−2.7	−2.5	−2.1	−3.9

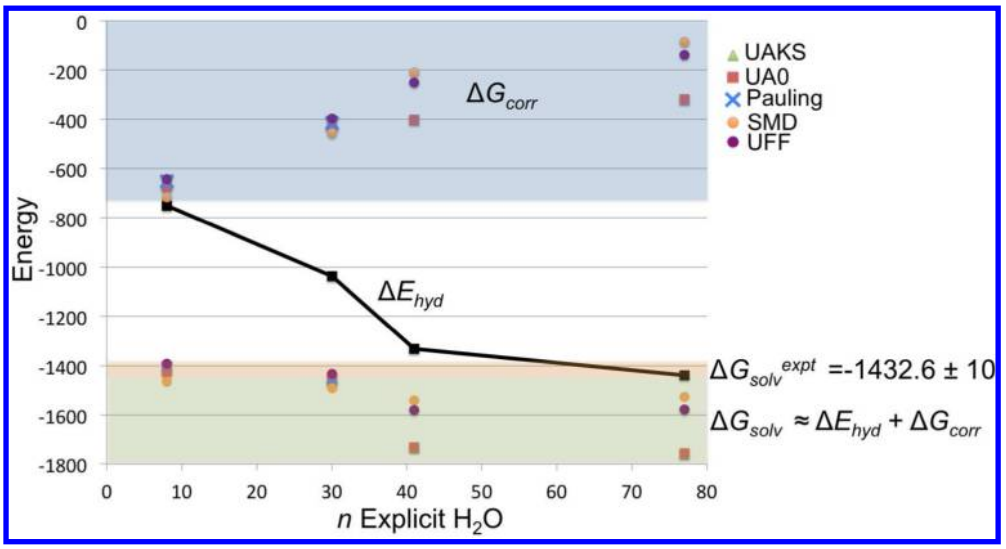

Figure 2. Calculated reaction energies (in kcal/mol) for reactions r1, r2, and r9 for U^{4+} in the gas-phase and in aqueous solution, determined using different dielectric continuum models. The experimental ΔG_{solv} is taken from refs 27 and 65.

The use of the uncontracted basis sets provides the opportunity to investigate the impact of spin−orbit (SO) coupling using the SO DFT formalism. The magnitude of SO coupling for the hydration reactions of all ions varies from 0.4−2.1 kcal/mol, indicating that the spin−orbit effects essentially cancel for the reactants and the products. The magnitude of the SO contribution to the hydration energies does not correlate well with the formal *f*-electron occupation (or oxidation states) for each ion, but it does correlate with the charge transfer and the effective *f*-electron occupation of the gas-phase cation vs the hydrated complexes for U^{4+} and UO_2^{2+}. The SO increases as the Lowdin charges decrease on ions (see Figure S4 in the Supporting Information). However, for U^{3+} and UO_2^{1+}, the change in the SO is almost neglible (0.4−1.0 kcal/mol) between the bare and hydrated ions. In the water addition reactions the difference in *f*-electron occupation of the metal is negligible between the reactants and products of the water addition reactions, and thus the SO contribution is essentially zero.

Solution-Phase Energetics: Performance of Polarizable Continuum Models Relative to Cluster Size. In its simplest form, the solution-phase correction to the gas-phase free energy of a species, G_{corr}, derives from three terms: 1) a free energy term associated with creation of a cavity around the solute, 2) a free energy contribution that results from dispersion-repulsion interactions between the cavity boundary and the dielectric continuum, and 3) an electrostatic free energy contribution between the cavity and the continuum:

$$G_{corr} = G_{cav} + G_{disp\text{-}rep} + G_{elec} \quad (2)$$

Both the IEF and SMD models employed in this work account for all three terms; however, by default the dispersion-repulsion term may not be included, and thus care must be taken to ensure consistency when comparing G_{corr} between different models and cavities. When considering the solution-phase correction for a chemical reaction, the total correction can be written as

$$\Delta G_{corr} = G_{corr}^{prod} - G_{corr}^{react} \quad (3)$$

Prior work has demonstrated that the solution-phase corrections obtained from polarizable continuum models for the hydration properties of lanthanides are not significantly influenced by the specific density functional used nor the basis set.[15] It is thus not surprising that neither uncontraction of the basis nor the addition of *g*-functions has a significant impact upon the solution-phase energetics for either the hydration reactions or the water addition reactions considered above (see Tables S2 and S3 in the Supporting Information). As such, within the remainder of this work the UB3LYP functional will be used in conjunction with the typically used RSC(1994) basis set, wherein comparisons are made between continuum models and cavities.

When considering the ability to calculate accurate free energies of solvation for ions, the error in ΔG_{solv} will be a composite of errors deriving from the gas-phase energetics as well as the solvation correction. Assuming that the intrinsic error in the gas-phase is minimized (as discussed above), the remaining error in the gas-phase hydration energy lies in the limited number of explicit waters of solvation. For clusters of

dx.doi.org/10.1021/ct500530q | J. Chem. Theory Comput. 2015, 11, 55−63

infinite size (the bulk limit), the ΔG_{hyd} is equivalent to ΔG_{solv} and ΔG_{corr} should go to zero as the G_{cav}, $G_{disp\text{-}rep}$, and G_{elec} of the reactants and products should cancel (eqs 1 − 3). The G_{elec} term in particular should approach zero for all species as the bulk limit is approached; however, this is not necessarily the case, and thus cancellation is desired. It is possible that the gas-phase ΔG_{hyd} and the solvation correction for the reaction, ΔG_{corr}, converge to the bulk limit at different rates with increasing explicit waters in the cluster (eq 1). It is then of interest to thoroughly examine the performance of the various dielectric continuum models and cavities as a function of the charge of the cluster and the convergence properties with increasing number of solvating waters. The latter is particularly important as our and other groups have reported vastly different calculated ΔG_{solv} values for metal ions depending upon the number of explicit waters in the cluster and the cavity employed.[16,64]

The convergence of the gas-phase hydration energy (ΔE_{hyd}) has been examined for U(IV), as described by reactions r1, r2, and r9, which consists of addition of U^{4+} to $(H_2O)_n$ clusters containing 8, 30, 41, and 77 water molecules. It is computationally impractical to perform complete geometry optimizations of the 41 and 77-H_2O clusters, thus single point calculations were performed and the convergence of ΔE_{hyd} was monitored. Similarly, the convergence of ΔG_{corr} was examined for each PCM employed, and then the sum of ΔE_{hyd} and ΔG_{corr} was plotted to approximate how the relative cancellation of errors in the two terms would impact a calculated ΔG_{solv} value (where $\Delta G_{solv} \approx \Delta E_{hyd} + \Delta G_{corr}$).

As seen in Figure 2, the gas-phase ΔE_{hyd} for the reaction converges nicely to the experimental value for ΔG_{solv} for U^{4+} since the explicit number of water molecules (n) about the ion is approaching the bulk. The slight bump in the convergence when transitioning from the n = 30 to n = 41 system is attributed to the fact that the n = 30 is the single configuration optimized with UB3LYP, while the energy of the n = 41 system represents the average of 5 single point energies of configurations obtained from MD. At a cluster size consisting of 77 water molecules ΔE_{hyd} is within the experimental error for ΔG_{solv}. As the size of the explicit water cluster is increased, the solvation corrections to the reaction energy should approach zero; however, it is apparent that in general the PCM convergence is significantly slower than that of ΔE_{hyd}.

Note that the nonelectrostatic contributions (ΔG_{cav} and $\Delta G_{disp\text{-}rep}$) to the ΔG_{corr} are essentially zero for the 41- and 77-water clusters, and thus it is the electrostatic contribution to ΔG_{corr} that does not approach zero fast enough for accurate ΔG_{solv} to be calculated even at a cluster size (77-waters) that includes what one could construe as a fourth solvation shell. While all cavities and models exhibit a large positive slope when going from the n = 8 to n = 30, the rate of convergence for UAKS and UA0 cavities dramatically drops off such that slopes of ∼2 are observed when transitioning from n = 41 to n = 77 molecular clusters. If this convergence rate is assumed to be constant as cluster size is increased, then the UAKS and UA0 cavities would not converge to a ΔG_{corr} value of zero until a cluster with at least 210 explicit waters was utilized (in reality the rate of convergence will decrease as n increases). In contrast, the UFF cavity within the IEF model and the SMD model maintain a faster rate of convergence until the n = 41 cluster size is reached. As such, the approximate size of hydrated metal ion cluster needed to reach the bulk solvation limit is only ∼100−120 explicit waters.

The difference in these convergence patterns can be further dissected by examination of the electrostatic contribution, G_{elec}, which is the dominant term in the solvation correction for the $(H_2O)_n$ reactants and the $U(H_2O)_n^{4+}$ products (eqs 2 and 3). This quantity has been plotted in Figure 3 for the SMD model

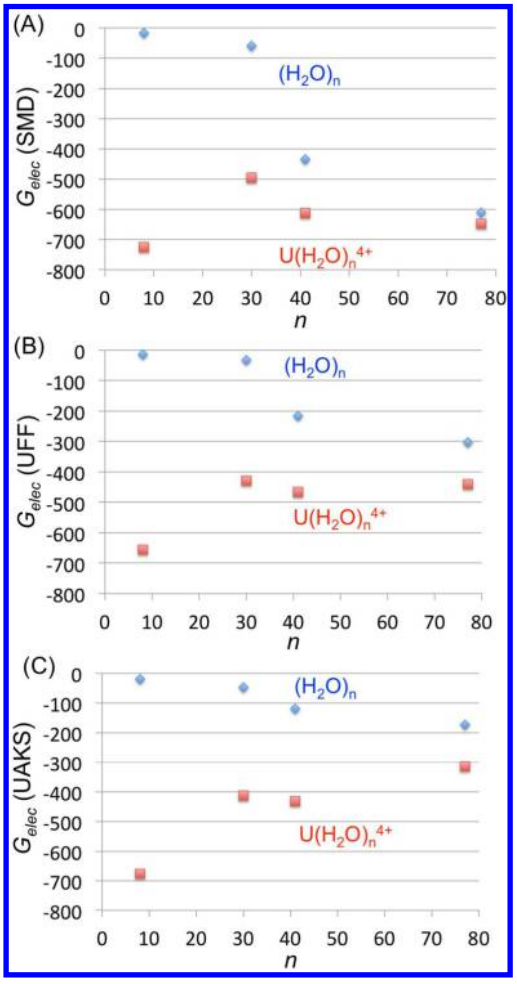

Figure 3. Electrostatic contribution, G_{elec}, (in kcal/mol) to the free energy of solvation correction for $(H_2O)_n$ reactant and $U(H_2O)_n^{4+}$ product clusters in the solvation reactions r1, r8, and r9 for (A) the SMD continuum model, (B) the UFF cavity within IEF, and (C) the UAKS cavity within the IEF model.

and the UFF and UAKS cavities within the IEF model. It should be first noted that in general the electrostatic contribution to the $(H_2O)_n$ reactant clusters becomes more negative as cluster size is increased, while the contribution to the products becomes less negative. This behavior is consistent with an increase in the amount of cancellation of G_{elec} of the products minus reactants and thus a general convergence of ΔG_{corr} toward zero. However, both the rate of change of G_{elec} and the values of G_{elec} specifically for the reactants and products differ in Figure 3. The G_{elec} of the metal ion using UAKS becomes less negative at a steady and nearly linear rate with a slope of +4, while at the same time the G_{elec} of the water cluster slowly becomes more negative with a slope of −2. There is thus an imbalance in the rates of change in the product and reactant electrostatic contributions to ΔG_{corr} which leads to a slow convergence of that quantity toward zero. Similar behavior is observed for UA0. The UFF cavity and SMD model exhibit less linear and more exponential behavior in G_{elec}. The ability of

dx.doi.org/10.1021/ct500530q | J. Chem. Theory Comput. 2015, 11, 55−63

ΔG_{corr} to approach zero in the bulk limit for SMD and UFF derives primarily from a steep increase in G_{elec} as the product cluster is increased from n = 8 to n = 30, while the reactant cluster G_{elec} becomes much more negative when n > 30. Thus, ΔG_{corr} approaches zero via the cancellation of much larger negative quantities than in UAKS.

The behavior of the G_{elec} term for the reactant $(H_2O)_n$ clusters is particularly important when considering less highly charged metal ions. As observed in Figure 4, the G_{elec} of the

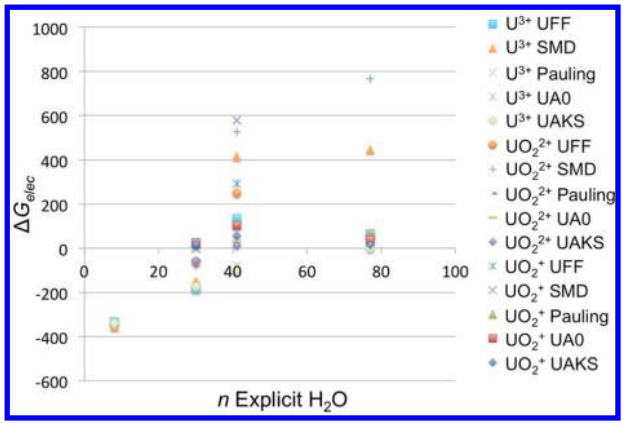

Figure 4. Electrostatic contribution, ΔG_{elec}, in kcal/mol to ΔG_{solv}, defined as $G_{elec}^{prod} - G_{elec}^{react}$.

product cluster can become less negative than G_{elec} of the water reactant cluster, leading to an unphysical positive ΔG_{elec} contribution to ΔG_{solv} (where $\Delta G_{elec} = G_{elec}^{prod} - G_{elec}^{react}$). As the total charge of the solute decreases, it becomes more likely for ΔG_{elec} to become positive. In turn, ΔG_{corr} may also become positive, and, importantly, it begins to diverge for the UAKS and UA0 cavities versus the SMD and UFF when using cluster models with more than two solvation shells (Figure 5). *Based upon the combined data presented in* Figures 2−5, *explicit water cluster models that utilize waters beyond a second solvation shell of the solute are not recommended for determining predictive thermochemistry for metal ions across a range of oxidation states.*

Given the constraint of smaller explicit water cluster models, it is worthwhile to discuss the means by which cancellation of errors can *fortuitiously* and possibly *consistently* lead to a ΔG_{solv} value in good agreement with experiment (eq 1). When a single solvation shell is present, the significantly underestimated gas-phase energy for the reaction must be compensated for by a large solvation correction. The latter is dominated by a negative ΔG_{elec} that is highly sensitive to the cavity volume and surface area. The error in the calculated ΔG_{solv} for $U(H_2O)_8^{4+/3+}$ relative to experiment ($\Delta G_{solv}^{expt} = -1432.6 \pm 10$ kcal/mol[65]) is plotted as a function of these parameters in Figure 6. First considering cavity volume, it is apparent that too small of a cavity volume leads to overestimated (too negative) ΔG_{solv} values but that the error in the solvation free energy trends approximately linearly with increasing volume. Interestingly, the errors when compared to cavity surface area do not trend linearly and too large a surface area can lead to either significant over- or underestimations of ΔG_{solv}. Importantly, those methods that produce the smallest cavity surface area do generally have the smallest errors with respect to experiment, including the traditional Pauling, UAKS, and UA0 methods. The UFF cavity has a large volume and large surface area, leading to underestimation of ΔG_{solv} for both tri- and

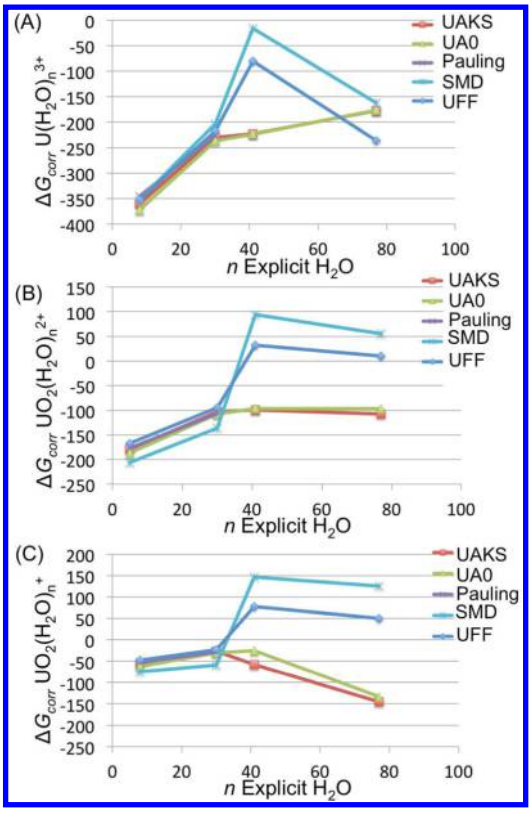

Figure 5. Convergences of the solution-phase correction to the free energy, ΔG_{corr}, for trivalent, hexavalent, and pentavalent uranium as a function of the size of the molecular hydrated cluster employed.

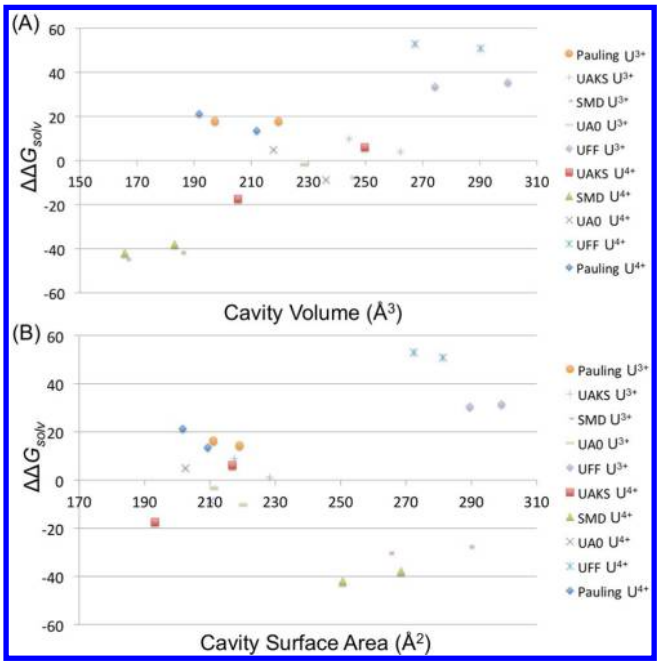

Figure 6. Comparison of the error in the calculated free energy of solvation ($\Delta\Delta G_{solv} = \Delta G_{solv}^{theory} - \Delta G_{solv}^{expt}$) in kcal/mol for both the 8- and 9- coordinated clusters of the form $U(H_2O)_{8,9}^{4+/3+}$ as a function of (A) cavity volume and (B) cavity surface area.

tetravalent uranium, while the SMD model results in small cavity volumes but larger surface areas, causing an over-estimated ΔG_{solv}. The net result of the sensitivity to cavity volume and surface area is an ∼140 kcal/mol range in the

dx.doi.org/10.1021/ct500530q | J. Chem. Theory Comput. 2015, 11, 55−63

Table 3. UB3LYP Calculated ΔG_{solv} Values (in kcal/mol) for U(III−VI) Using Reactions r1−r4 Calculated in Aqueous Solution[e]

	$U^{4+} + (H_2O)_{n+m} \rightarrow U(H_2O)_n(H_2O)_m^{4+}$		$U^{3+} + (H_2O)_{n+m} \rightarrow U(H_2O)_n(H_2O)_m^{3+}$		$UO_2^{2+} + (H_2O)_{n+m} \rightarrow UO_2(H_2O)_n(H_2O)_m^{2+}$		$UO_2^{+} + (H_2O)_{n+m} \rightarrow UO_2(H_2O)_n(H_2O)_m^{+}$	
	n, m = 8,0	n, m = 9,0	n, m = 8,0	n, m = 9,0	n, m = 4,0	n, m = 5,0	n, m = 4,0	n, m = 5,0
UAKS	−1450.0	−1426.4	−765.0	−772.7	−363.4	−373.1	−269.4	−270.6
UA0	−1427.7	−1441.3	−776.8	−783.7	−370.1	−380.5	−273.9	−276.6
Pauling	−1411.4	−1419.0	−757.6	−759.5	−369.7	−370.7	−271.0	−267.5
SMD	−1474.6	−1470.5	−804.1	−801.4	−400.5	−400.0	−293.9	−289.1
UFF	−1379.4	−1381.6	−743.4	−742.4	−357.5	−360.8	−265.1	−262.2
	n,m = 8, 22	n, m = 9, 21	n, m = 8, 22	n, m = 9, 21	n, m = 4, 26	n, m = 5, 25	n, m = 4, 26	n, m = 5, 25
UAKS	−1459.6	−1468.7	−782.9	−787.8	−390.2	−397.9	−258.9	−264.0
UA0	−1468.8	−1477.2	−790.7	−794.5	−392.0	−402.7	−260.8	−268.7
Pauling	−1459.2	−1464.0	−780.2	−783.8	−397.6	−401.3	NA[d]	−288.7
SMD	−1477.6	−1479.6	−794.6	−789.7	−417.5	−412.1	−283.2	−278.0
UFF	**−1437.9**	**−1436.7**	**−766.9**	**−761.6**	**−387.4**	**−389.7**	**−259.7**	**−260.8**
expt[a,b,c]	**−1432.6 ± 10**		**−773.9 ± 10**		**−397 ± 15**			

[a]Reference 65. [b]Reference 27. [c]Reference 66. [d]Unable to converge Pauling SCF energy. [e]The UFF cavity values are in bold so as highlight their consistently good performance when a second solvation shell is employed.

predicted ΔG_{solv} values for tri- and tetravalent uranium as seen in Table 3.

When a second solvation shell is added, the gas-phase reaction energy drops significantly toward the infinite bulk limit. At the same time the presence of a second shell of solvating waters decreases the electrostatic interactions on the cavity surface, and thus the sensitivity of the calculated ΔG_{solv} upon the cavity and model employed. As such, the standard deviation in the theoretical ΔG_{solv} for all methods drops in half when a second solvation shell is added (Table 3). The slopes of ΔG_{corr} between the $U(H_2O)_8^{4+}$ and $U(H_2O)_8(H_2O)_{22}^{4+}$ data points in Figure 2 are between 3.0−4.0, which is nearly half that of ΔE_{hyd} (slope of 7.6). Thus, those cavities which started off in $U(H_2O)_8^{4+}$ with a smaller calculated ΔG_{corr} are benefitted in the second solvation shell cluster by less overcancellation of the error in ΔE_{hyd}. As such, the UFF cavity yields ΔG_{solv} values that are in very good agreement with experimental data for uranium across all oxidation states when a second solvation shell is present. Based upon the information obtained from the convergence properties of the different contributions to ΔG_{corr} it is apparent that good performance for this cavity derives from a consistent cancellation of the errors contained in the electrostatic contribution to ΔG_{corr} and ΔE_{hyd}. Based upon these data we suggest further exploration of the UFF cavity as one that can consistently yield accurate solution-phase energetics of metal ions of varying oxidation state.

CONCLUSIONS

The work herein demonstrates that PCMs can be an effective approach for determining consistently accurate free energies of solvation for metal cations across multiple oxidation states. However, this conclusion derives from a deeper understanding of the contributions to the solvation correction for both reactants and products in the hydration reaction of a bare ion. In particular, the cancellation of errors in the gas-phase and solvation corrections must be appreciated as the fundamental factor necessary for obtaining an accurate ΔG_{solv}. Different cavities (UAKS, UFF, UA0, Pauling) and models (IEF and SMD) exhibit very different convergence properties as a function of the number of explicit solvating molecules in the molecular cluster, and this is believed to be the primary source behind previous discrepancies in ΔG_{solv} as a function of PCM cavity and model. Thus, extreme care must be taken when choosing a molecular cluster size, cavity, and model within the computational protocol for determining the solution-phase thermochemistry. The UFF cavity is demonstrated to result in consistent and fortuitous cancellation of errors when determining the ΔG_{solv} for U(III−VI) using molecular clusters that consist of a second solvation shell.

ASSOCIATED CONTENT

Supporting Information

Further tables with information about the basis set and spin−orbit affects upon calculated thermodynamic values and Cartesian coordinates of relevant structures. This material is available free of charge via the Internet at http://pubs.acs.org.

AUTHOR INFORMATION

Corresponding Authors

*E-mail: payal.parmar@wsu.edu.

*E-mail: auclark@wsu.edu.

Notes

The authors declare no competing financial interest.

ACKNOWLEDGMENTS

An award of computer time was provided by the Innovative and Novel Computational Impact on Theory and Experiment (INCITE) program. This research used resources of the Oak Ridge Leadership Computing Facility located in the Oak Ridge National Laboratory, which is supported by the Office of Science of the Department of Energy under Contract DE-AC05-00OR22725. Research in the authors' laboratory is funded by the National Science Foundation, award #: 0848346.

REFERENCES

(1) Miertus, S.; Scrocco, E.; Tomasi, J. *Chem. Phys.* **1981**, *55*, 117.
(2) Cramer, C. J.; Truhlar, D. G. *Chem. Rev.* **1999**, *99*, 2161.
(3) Tomasi, J. *ACS Symp. Ser.* **1994**, *568*, 10.
(4) Cossi, M.; Scalmani, G.; Rega, N.; Barone, V. *J. Chem. Phys.* **2002**, *117*, 43.
(5) Tomasi, J.; Mennucci, B.; Cammi, R. *Chem. Rev.* **2005**, *105*, 2999.
(6) Takano, Y.; Houk, K. N. *J. Chem. Theory Comput.* **2005**, *1*, 70.
(7) Cossi, M.; Barone, V.; Mennucci, B.; Tomasi, J. *Chem. Phys. Lett.* **1998**, *286*, 253.

(8) Dolney, D. M.; Hawkins, G. D.; Winget, P.; Liotard, D. A.; Cramer, C. J.; Truhlar, D. G. *J. Comput. Chem.* **2000**, *21*, 340.
(9) Li, J. B.; Zhu, T. H.; Cramer, C. J.; Truhlar, D. G. *J. Phys. Chem. A* **2000**, *104*, 2178.
(10) Barone, V.; Cossi, M.; Tomasi, J. *J. Chem. Phys.* **1997**, *107*, 3210.
(11) Richens, D. T. *The chemistry of aqua ions: synthesis, structure, and reactivity*; Wiley: Chichester, U.K., 1997; p 2.
(12) Martinez, J. M.; Pappalardo, R. R.; Marcos, E. S.; Mennucci, B.; Tomasi, J. *J. Phys. Chem. B* **2002**, *106*, 1118.
(13) Tunon, I.; Rinaldi, D.; Ruizlopez, M. F.; Rivail, J. L. *J. Phys. Chem.* **1995**, *99*, 3798.
(14) Gutowski, K. E.; Dixon, D. A. *J. Phys. Chem. A* **2006**, *110*, 8840.
(15) Dinescu, A.; Clark, A. E. *J. Phys. Chem. A* **2008**, *112*, 11198.
(16) Gutowski, K. E.; Dixon, D. A. *J. Phys. Chem. A* **2006**, *110*, 8840.
(17) Cramer, C. J.; Truhlar, D. G. *Science* **1992**, *256*, 213.
(18) Miertus, S.; Tomasi, J. *Chem. Phys.* **1982**, *65*, 239.
(19) Mohan, V.; Davis, M. E.; Mccammon, J. A.; Pettitt, B. M. *J. Phys. Chem.* **1992**, *96*, 6428.
(20) Still, W. C.; Tempczyk, A.; Hawley, R. C.; Hendrickson, T. *J. Am. Chem. Soc.* **1990**, *112*, 6127.
(21) Curutchet, C.; Orozco, M.; Luque, F. J. *J. Comput. Chem.* **2001**, *22*, 1180.
(22) Giesen, D. J.; Hawkins, G. D.; Liotard, D. A.; Cramer, C. J.; Truhlar, D. G. *Theor. Chem. Acc.* **1997**, *98*, 85.
(23) Li, J. B.; Zhu, T. H.; Hawkins, G. D.; Winget, P.; Liotard, D. A.; Cramer, C. J.; Truhlar, D. G. *Theor. Chem. Acc.* **1999**, *103*, 9.
(24) Luque, F. J.; Bachs, M.; Aleman, C.; Orozco, M. *J. Comput. Chem.* **1996**, *17*, 806.
(25) Luque, F. J.; Zhang, Y.; Aleman, C.; Bachs, M.; Gao, J.; Orozco, M. *J. Phys. Chem.* **1996**, *100*, 4269.
(26) Sitkoff, D.; BenTal, N.; Honig, B. *J. Phys. Chem.* **1996**, *100*, 2744.
(27) *Handbook on the Physics and Chemistry of Rare Earths. Volume 18: Lanthanides/Actinides: Chemistry*; Rizkalla, E. N., Choppin, G. R., Gschneider, K. A., Jr., Eyring, L., Lander, G. H., Eds.; North-Holland: New York, 1994; Vol. *18*, p 529.
(28) Vyacheslav, S. B.; Diallo, M. S.; Goddard, W. A. *J. Phys. Chem. B* **2008**, *112*, 9709.
(29) Asthagiri, D.; Pratt, L. R.; Ashbaugh, H. S. *J. Chem. Phys.* **2003**, *119*, 2702.
(30) Ben-Naim, A. *J. Phys. Chem.* **1987**, *82*, 792.
(31) Grabowski, P.; Riccardi, D.; Gomez, M. A.; Asthagiri, D.; Pratt, L. R. *J. Phys. Chem. A* **2002**, *106*, 9145.
(32) Pliego, J. R., Jr.; Riveros, J. M. *J. Phys. Chem. A* **2001**, *105*, 7241.
(33) Clark, A. E. *J. Chem. Theory Comput.* **2008**, *4*, 708.
(34) Schreckenbach, G.; Shamov, G. A. *Acc. Chem. Res.* **2010**, *43*, 19.
(35) Shamov, G. A.; Schreckenbach, G. *J. Phys. Chem. A* **2005**, *109*, 10961.
(36) Batista, E. R.; Martin, R. L.; Hay, P. J.; Peralta, J. E.; Scuseria, G. E. *J. Chem. Phys.* **2004**, *121*, 2144.
(37) Schreckenbach, G.; Hay, P. J.; Martin, R. L. *J. Comput. Chem.* **1999**, *20*, 70.
(38) Mattsson, A. E. *Science* **2002**, *298*, 759.
(39) Perdew, J. P.; Schmidt, K. In *Density Functional Theory and its Application to Materials*; Van Doren V. E., Van Alsenoy, C., Geerlings, P., Eds.; AIP: Melville, NY, 2001; p 5.
(40) Kuta, J.; Clark, A. E. *Inorg. Chem.* **2010**, *49*, 7808.
(41) Pyykko, P.; Li, J.; Runeberg, N. *J. Phys. Chem.* **1994**, *98*, 4809.
(42) Becke, A. D. *J. Chem. Phys.* **1993**, *98*, 5648.
(43) Lee, C. T.; Yang, W. T.; Parr, R. G. *Phys. Rev. B* **1988**, *37*, 785.
(44) Valiev, M.; Bylaska, E. J.; Govind, N.; Kowalski, K.; Straatsma, T. P.; van Dam, H. J. J.; Wang, D.; Nieplocha, J.; Apra, E.; Windus, T. L.; de Jong, W. A. *Comput. Phys. Commun.* **2010**, *181*, 1477.
(45) Kuchle, W.; Dolg, M.; Stoll, H.; Preuss, H. *J. Chem. Phys.* **1994**, *100*, 7535.
(46) Dolg, M.; Cao, X. Y. *J. Phys. Chem. A* **2009**, *113*, 12573.
(47) Dunning, T. H., Jr. *J. Chem. Phys.* **1989**, *90*, 1007.
(48) Kvamme, B.; Wander, M. C. F.; Clark, A. E. *Int. J. Quantum Chem.* **2009**, *109*, 2474.
(49) Frisch, M. J.; Trucks, G. W.; Schlegel, H. B.; Scuseria, G. E.; Robb, M. A.; Cheeseman, J. R.; Montgomery, J. A., Jr.; Vreven, T.; Kudin, K. N.; Burant, J. C.; Millam, J. M.; Iyengar, S. S.; Tomasi, J.; Barone, V.; Mennucci, B.; Cossi, M.; Scalmani, G.; Rega, N.; Petersson, G. A.; Nakatsuji, H.; Hada, M.; Ehara, M.; Toyota, K.; Fukuda, R.; Hasegawa, J.; Ishida, M.; Nakajima, T.; Honda, Y.; Kitao, O.; Nakai, H.; Klene, M.; Li, X.; Knox, J. E.; Hratchian, H. P.; Cross, J. B.; Bakken, V.; Adamo, C.; Jaramillo, J.; Gomperts, R.; Stratmann, R. E.; Yazyev, O.; Austin, A. J.; Cammi, R.; Pomelli, C.; Ochterski, J. W.; Ayala, P. Y.; Morokuma, K.; Voth, G. A.; Salvador, P.; Dannenberg, J. J.; Zakrzewski, V. G.; Dapprich, S.; Daniels, A. D.; Strain, M. C.; Farkas, O.; Malick, D. K.; Rabuck, A. D.; Raghavachari, K.; Foresman, J. B.; Ortiz, J. V.; Cui, Q.; Baboul, A. G.; Clifford, S.; Cioslowski, J.; Stefanov, B. B.; Liu, G.; Liashenko, A.; Piskorz, P.; Komaromi, I.; Martin, R. L.; Fox, D. J.; Keith, T.; Al-Laham, M. A.; Peng, C. Y.; Nanayakkara, A.; Challacombe, M.; Gill, P. M. W.; Johnson, B.; Chen, W.; Wong, M. W.; Gonzalez, C.; Pople, J. A. *Gaussian 03*, Revision C.02; Gaussian, Inc.: Wallingford, CT, 2004.
(50) Pascual-Ahuir, J. L.; Silla, E.; Tunon, I. *J. Comput. Chem.* **1994**, *15*, 1127.
(51) Tomasi, J.; Mennucci, B.; Cances, E. *J. Mol. Struct.: THEOCHEM* **1999**, *464*, 211.
(52) Frisch, M. J.; Trucks, G. W.; Schlegel, H. B.; Scuseria, G. E.; Robb, M. A.; Cheeseman, J. R.; Scalmani, G.; Barone, V.; Mennucci, B.; Petersson, G. A.; Nakatsuji, H.; Caricato, M.; Li, X.; Hratchian, H. P.; Izmaylov, A. F.; Bloino, J.; Zheng, G.; Sonnenberg, J. L.; Hada, M.; Ehara, M.; Toyota, K.; Fukuda, R.; Hasegawa, J.; Ishida, M.; Nakajima, T.; Honda, Y.; Kitao, O.; Nakai, H.; Vreven, T.; Montgomery, J. A., Jr.; Peralta, J. E.; Ogliaro, F.; Bearpark, M.; Heyd, J. J.; Brothers, E.; Kudin, K. N.; Staroverov, V. N.; Kobayashi, R.; Normand, J.; Raghavachari, K.; Rendell, A.; Burant, J. C.; Iyengar, S. S.; Tomasi, J.; Cossi, M.; Rega, N.; Millam, M. J.; Klene, M.; Knox, J. E.; Cross, J. B.; Bakken, V.; Adamo, C.; Jaramillo, J.; Gomperts, R.; Stratmann, R. E.; Yazyev, O.; Austin, A. J.; Cammi, R.; Pomelli, C.; Ochterski, J. W.; Martin, R. L.; Morokuma, K.; Zakrzewski, V. G.; Voth, G. A.; Salvador, P.; Dannenberg, J. J.; Dapprich, S.; Daniels, A. D.; Farkas, Ö.; Foresman, J. B.; Ortiz, J. V.; Cioslowski, J.; Fox, D. J. *Gaussian 09*, Revision D.01; Gaussian, Inc.: Wallingford, CT, 2009.
(53) Marenich, A. V.; Cramer, C. J.; Truhlar, D. G. *J. Phys. Chem. B* **2009**, *113*, 6378.
(54) Yang, T.; Bursten, B. *Inorg. Chem.* **2006**, *45*, 5291.
(55) Jorgensen, W. L.; Chandrasekhar, J.; Madura, J. D.; Impey, R. W.; Klein, M. L. *J. Chem. Phys.* **1983**, *79*, 926.
(56) Waldher, B.; Kuta, J.; Chen, S.; Henson, N.; Clark, A. E. *J. Comput. Chem.* **2010**, *31*, 2307.
(57) Smith, W.; Todorov, I. T. *Mol. Sim.* **2006**, *32*, 935.
(58) Smith, W.; Todorov, I. T.; Leslie, M. *Z. Kristallogr.* **2005**, *220*, 563.
(59) Todorov, I. T.; Smith, W.; Trachenko, K.; Dove, M. T. *J. Mater. Chem.* **2006**, *16*, 1911.
(60) Ozkanlar, A.; Clark, A. E. *J. Comput. Chem.* **2014**, *35*, 495.
(61) Vallet, V.; Schimmelpfennig, B.; Maron, L.; Teichteil, C.; Leininger, T.; Gropen, O.; Grenthe, I.; Wahlgren, U. *Chem. Phys.* **1999**, *244*, 185.
(62) Garcia-Hernandez, M.; Lauterbach, C.; Kruger, S.; Matveev, A.; Rosch, N. *J. Comput. Chem.* **2002**, *23*, 834.
(63) Straka, M.; Kaupp, M. *Chem. Phys.* **2005**, *311*, 45.
(64) Kuta, J.; Wander, M. C. F.; Wang, Z. M.; Jiang, S. D.; Wall, N. A.; Clark, A. E. *J. Phys. Chem. C* **2011**, *115*, 21120.
(65) Bratsch, S. G.; Lagowski, J. J. *J. Phys. Chem.* **1986**, *90*, 307.
(66) Gibson, J. K.; Haire, R. G.; Santos, M.; Marcalo, J.; de Matos, A. P. *J. Phys. Chem. A* **2005**, *109*, 2768.